Influence of Temperature-Dependent Resin Behavior on Numerical Prediction of Effective CTEs of 3D Woven Composites

KOSTIANTYN VASYLEVSKYI, BORYS DRACH
and IGOR TSUKROV

ABSTRACT

3D woven composites are well known for their high strength, dimensional stability, delamination, and impact resistance. They are often used in aerospace, energy, and automotive industries where material parts can experience harsh service conditions including substantial variations in temperature. This may lead to significant thermal deformations and thermally-induced stresses in the material. Additionally, 3D woven composites are often produced using resin transfer molding (RTM) technique which involves curing the epoxy resin at elevated temperatures leading to accumulation of the processing-induced residual stress. Thus, understanding of effective thermal behavior of 3D woven composites is essential for their successful design and service.

In this paper, the effective thermal properties of 3D woven carbon-epoxy composite materials are estimated using mesoscale finite element models previously developed for evaluation of the manufacturing-induced residual stresses. We determine effective coefficients of thermal expansion (CTEs) of the composites in terms of the known thermal and mechanical properties of epoxy resin and carbon fibers. We investigate how temperature sensitivity of the thermal and mechanical properties of the epoxy influences the overall thermal properties of the composite. The simulations are performed for different composite reinforcement morphologies including ply-to-ply and orthogonal. It is shown that even linear dependence of epoxy's stiffness and CTE on temperature results in a nonlinear dependence on temperature of the overall composite's CTE.

Kostiantyn Vasylevskyi, Igor Tsukrov: University of New Hampshire, Department of Mechanical Engineering, 33 Academic Way, Durham, NH 03824, U.S.A.
Borys Drach: New Mexico State University, Department of Mechanical and Aerospace Engineering, 1040 S. Horseshoe Str., Las Cruces, NM 88003, U.S.A.

INTRODUCTION

3D woven composite materials are broadly used in aerospace, energy and automotive industries owing to their high strength, light weight, impact and delamination resistance which distinguish them from other textile and laminated composite materials [1]. These materials often experience challenging service conditions such as impact loadings [2], cyclic loadings [3], [4] and significant variation in service temperature [5] and [6]. Thus, it becomes crucial to determine effective coefficients of thermal expansion (CTEs). There are many publications dedicated to the analytical micromechanical predictions of the effective coefficients of thermal expansion of composites. A comprehensive discussion of analytical approaches to predict CTEs for various microstructures can be found in [7]. However, when the microstructure of a composite material is of a complex woven morphology, obtaining analytical solutions for the homogenization of thermo-mechanical properties may not be possible. Then a direct FE modeling approach can be used. For example, Tan *et al.* [8] predicted effective CTEs of 3D woven carbon/epoxy composites. Ai *et al*. [9] calculated effective CTEs of carbon/carbon composites at high temperatures reporting temperature dependent effective CTEs of the composite as compared to the experimental measurements published in Wang *et al*. [10]. Dong *et al*. [11] predicted effective CTEs of carbon/epoxy plain woven composites, the authors reported temperature dependent CTEs of the composite and compared the numerical predictions with the experimental data. Gou *et al*. [12] performed similar numerical studies predicting effective CTEs of plain weave composites. Siddgonde and Gosh [13] evaluated effective CTEs of 3D woven carbon/carbon composites, the effective CTEs were presented as functions of temperature, and the impact of the fabrics reinforcement morphology on the effective CTEs was investigated.

Often, carbon/epoxy composites are produced using resin transfer molding (RTM) technique which implies curing of the epoxy resin phase at elevated temperatures. Since CTE of resin is higher than CTE of fiber, this leads to an accumulation of residual stresses and strains in the material when it is cooled down. The state of the material when it has zero thermal strains is usually called the reference state and the temperature where this reference state exists is a reference temperature. There is no agreement in the literature on whether the reference state of the material has to be taken into account during effective CTE determination using mesoscale FE modeling. For example, authors in [8], [9], [13], and [14] performed their numerical calculations assuming that the reference state of the composite exists at each given level of temperature, whereas authors in [11] and [12] took into account the fact of reference temperature being different from the temperature of interest.

In this work, we investigate the effect of the reference temperature being different from the temperature of interest on the prediction of the effective CTE of 3D woven carbon/epoxy composites with temperature dependent thermo-mechanical properties of the constituents. We also demonstrate how mesoscale FE models developed for prediction of the residual stress accumulation in the 3D woven composites (see for example [15], and [16]) are used to determine effective CTEs. We propose a simple and efficient way to account for the reference state of the composite in the calculation of the effective CTEs.

The paper is organized as follows. Mesoscale modeling approach is described in the first section which includes information on micromechanical homogenization

procedure of the tow phase, FE models development, and application of boundary conditions. Various effective CTEs determination techniques are also discussed. The second section presents the effect of the temperature dependence of the constituents' properties on the effective CTEs of the composite for the composite with simplified reinforcement architecture and the actual as-woven fabrics. The third section provides conclusions of this research.

MESO-SCALE MODELING APPROACH

Finite Element Models Development

As fabric reinforcements in textile composites are periodic, only the smallest repeatable portion of the material – unit cell (UC) – is needed to be modeled to predict composite's effective properties. The outline of the procedure, published earlier in [17], is as follows.

The process starts with development of the geometric representation of the reinforcement. There are multiple different approaches to model the reinforcement, e.g. [18], [19], [20] and [21]. In our models we adapted the approach published in [22] and used Digital Fabric Mechanics Analyzer (DFMA) software to obtain as-woven geometric representation of the reinforcement architecture.

Next step is to produce a finite element mesh representing the reinforcement and matrix phase of the composite. The mesh for the reinforcement is created based on the geometric data obtained from DFMA. For the matrix phase, it is generated by filling the space between the reinforcement tows and creating flat top and bottom surfaces of the composite plate. Note that we neglect possible defects in the matrix and/or tows, such as pores, cracks and discontinuity at the interface between matrix and reinforcement phases, assuming that each composite phase is homogeneous and the contact between the tows and matrix is perfect.

The resulting finite element mesh needs to be periodic (compatible on the opposite sides of the UC). This requirement is imposed by application of the periodic boundary conditions (PBCs) which are usually used in the woven composites modeling to preserve continuity of the material, e.g. [19], [23], [24]. The 2D in-plane periodicity for a woven plate is formulated as:

$$u_i^+ = u_i^- + \delta_i, \text{ (i=}x \text{ (warp)}, y \text{ (weft)}) \quad (1)$$

where $\underline{u_i^+}$ and $\underline{u_i^-}$ are the nodal displacements on the opposite faces of the unit cell (positive and negative, respectively) and δ_i is an average displacement in i^{th} direction. Note that the unit cell represents the entire thickness of the composite plate, so only in-plane periodicity needs to be enforced.

Micromechanical Modeling of the Tows

In our simulations, we treat the reinforcement tows (aligned carbon fibers impregnated with epoxy resin) as a transversely isotropic unidirectional composite material. One of the commonly-used micromechanical approaches to predict elastic

properties of the tows by using Chamis formulae [25]. However, as it has been shown in [26] and [27], Chamis approach may lead to the effective properties exceeding the rigorous Hashin-Shtrikman bounds, [28]. Thus, in our modeling we used a combination of different approaches to perform homogenization of the mechanical and thermal properties of the tows. Longitudinal Young's E_1 modulus and Poisson's ratio v_{12} were obtained using Chamis formulae and transverse Young's modulus E_2, shear modulus G_{12} and Poisson's ratio in the transverse plane v_{23} were obtained using Hashin approach, see [29]. Explicit expressions for the effective elastic properties and more detailed description of the micromechanical modeling in our research is provided in [15].

In addition to effective elastic properties of the tows, their effective CTEs must be calculated. In this paper we use formulae provided in [30] to calculate longitudinal CTE of the tows:

$$\alpha_{1t} = \frac{E_{1f}\alpha_{1f}V_f + E_m\alpha_m V_m}{E_{1f}V_f + E_m V_m}, \quad (2)$$

where E_{1f} is the longitudinal Young's modulus, α_{1f} is the longitudinal CTE and V_f is the volume fraction of the fibers. E_m, α_m and V_m are Young's modulus, CTE and volume fraction of epoxy resin. To calculate transverse CTE we use expressions given in [29]:

$$\alpha_{2t} = \alpha_{2f}V_f\left(1 + v_{12f}\frac{\alpha_{1f}}{\alpha_{2f}}\right) + \alpha_m V_m(1 + v_m) - (v_{12f}V_f + v_m V_m)\alpha_{1t}, \quad (3)$$

where α_{2f}, v_{12f} are the transverse CTE and Poisson's ratio of the fibers and v_m is the Poisson's ration of the resin.

Thermo-mechanical Properties of the Matrix Phase

In our meso-scale models, we simulate matrix phase as homogeneous isotropic solid with temperature dependent Young's modulus E_m and CTE α_m and constant Poisson's ratio v_m. Both Young's modulus and CTE of epoxy are expressed as linear functions of temperature [31]:

$$E_m = E_m^{0^oC} - \beta_m T, \quad (4)$$

$$\alpha_m = \alpha_m^{0^oC} - \gamma_m T, \quad (5)$$

where T is temperature in ^{o}C, and $E_m^{0^oC}$, $\alpha_m^{0^oC}$, β_m and γ_m are the material parameters.

Effective CTE calculation process

According to [32], there are three general approaches to obtain effective CTE $\overline{\boldsymbol{\alpha}}$ of a composite material using finite element models of a composite unit cell. The first approach is to calculate effective CTEs using displacements of the control nodes used

in the definition of the periodic boundary conditions. For this approach, the periodic boundary conditions are combined with zero-traction on the faces of the UC and a finite uniform temperature change of ΔT is applied to the UC. In this case effective CTEs are given as follows:

$$\overline{\alpha}_i = \frac{1}{\Delta T}\frac{\delta_i}{L_i}, (i=1, 2, 3) \tag{6}$$

where $\overline{\alpha}_i$is the effective CTE in i^{th} direction, δ_i is the displacement of the control node due to the uniform temperature change ΔT, and L_i is the UC size in the i^{th} direction. However, this approach does not allow to calculate CTEs in all three directions if the periodicity is not enforced in all three directions, as, for example, in the case of considered 3D woven composites with in-plane periodicity. Additionally, such an approach makes it difficult to determine nondiagonal components of the CTE tensor in a general case.

The second approach allows to calculate the effective CTE by expressing it in terms of the average strain $\langle \boldsymbol{\varepsilon} \rangle$ accumulated in the UC due to a uniform temperature change ΔT. Similarly to the first approach, the periodicity is imposed to the unit cell and zero traction is prescribed to the UC faces allowing the material to freely deform due to the temperature change. Then the components of the average thermal strain are calculated as follows:

$$\langle \varepsilon_{ij} \rangle = \frac{1}{V_{UC}} \sum_{n=1}^{N} \left(\varepsilon_{ij}\right)_n V_n, (i,j=1, 2, 3) \tag{7}$$

where V_{UC} is the volume of the UC, $\left(\varepsilon_{ij}\right)_n$ is the local thermal strain component in the centroid of n^{th} finite element, V_n is the element's volume, and N is the number of finite elements in the UC. The effective CTEs are then expressed as follows:

$$\overline{\alpha}_{ij} = \frac{1}{\Delta T}\langle \varepsilon_{ij} \rangle. \tag{8}$$

This approach allows to obtain all the components of the effective CTE tensor. However, the calculation of the average strain may be computationally expensive, especially for the UCs modeled with a significant number of finite elements.

The third approach is to calculate effective CTEs by applying uniform temperature change ΔT to the UC with zero macroscopic strains prescribed. Such a loadcase leads to accumulation of the thermally-induced stresses within the material. Calculating the components of average stress $\langle \sigma_{ij} \rangle$ similarly to eq. (7), the effective CTEs can be obtained as follows:

$$\overline{\alpha_{ij}} = -\frac{1}{\Delta T}\overline{S}_{ijkl}\langle \sigma_{kl} \rangle, \tag{9}$$

where $\overline{S}_{ijkl}$ are the components the effective compliance tensor of the composite material. To use this approach, the effective compliance tensor of the composite has to be calculated prior to the thermal analysis. The effective compliance tensor calculation technique is presented, for example, in [33]. The fact that the effective elastic properties are required to calculate CTEs, makes this approach more

computationally challenging and time consuming as compared to the previous methods.

Note that if material properties of the constituents are temperature-dependent, the calculation of the effective CTE using equations (6), (8) or (9) must be carried out at each value of temperature of interest.

In this paper, the second approach to calculate effective CTE tensor (average macroscopic strain) is used. The same approach was used in [14] for the direct FEA approach to predict effective CTE of the composite.

PREDICTION OF THE CTES FOR TEMPERATURE-DEPENDENT MATRIX COMPOSITE

As 3D woven composite material constituents often exhibit temperature-dependent material properties ([31], [34]) and can be manufactured at elevated temperature, the effective thermal expansion/contraction behavior of the composite might become nonlinear with respect to temperature even if the properties of the phases are linearly dependent on temperature. In this case the conventional approaches to determine effective CTEs described in the previous section might become inaccurate.

Illustration by a simple model

To provide an illustration, a model of the layered composite material unit cell is considered, see Figure 1. The geometric size of this unit cell is 1mm×1mm×1mm and it is meshed using 1000 hexahedral linear finite elements. Periodic boundary conditions are applied in 1~2 plane.

The outer layers denoted as “matrix” are modeled as HEXCEL RTM6 epoxy resin and the inner layer (“reinforcement”) phase is as IM7 carbon fibers impregnated with RTM6 epoxy. The volume fraction of the reinforcement is V_f=0.2. Elastic moduli and CTEs of the reinforcement phase are shown in TABLE I. The reinforcement material is assumed to be transversely isotropic, with the transverse symmetry axis coinciding with global coordinate axis 1.

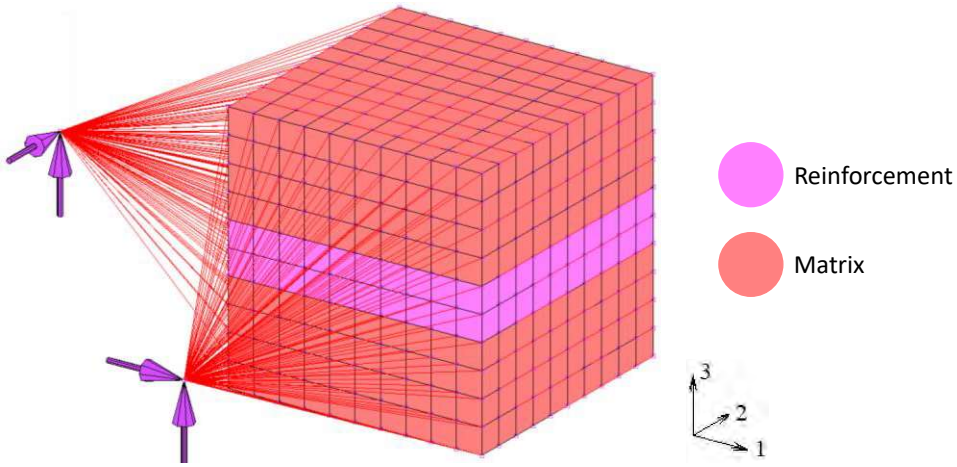

Figure 1. FE model of a simple composite RVE with periodic boundary conditions applied.

TABLE I. Elastic moduli and CTEs of IM7 carbon fibers impregnated with RTM6 epoxy resin.

E_1, MPa	$E_{2,3}$, MPa	ν_{12}	ν_{31}	G_{12}, MPa	α_1	α_2
221378	13180.2	0.35	0.020838	7171.7	-2.423 × 10^{-7}	2.1 × 10^{-5}

While material properties of the tows are temperature independent (the thermal sensitivity has shown to be negligible, see [15]), elastic modulus and CTE of RTM6 are linear functions of temperature and are defined by equations (4) and (5) with coefficients given in TABLE II. The Poisson's ratio of this epoxy is $\nu_m = 0.35$.

To determine, whether the conventional approach to predict effective CTEs is applicable for composites with temperature-dependent properties of constituents, the instantaneous effective CTEs need to be calculated as a derivative of the thermal strains with respect to temperature:

$$\alpha_{ij} = \frac{\partial\langle\varepsilon_{ij}\rangle}{\partial T}, \text{ (i, j = 1, 2, 3)} \tag{10}$$

and compared to the values of $\bar{\alpha}_{ij}$ obtained using equation (6), (8) or (9) when ΔT is small. Note that the derivatives are taken using finite backward difference approach. For the considered unit cell with transversely isotropic reinforcement phase material, the homogenized elastic properties are orthotropic and nondiagonal components of effective CTE tensor $\boldsymbol{\alpha}$ are zero.

Mean CTEs $\bar{\alpha}_1(T)$ and $\bar{\alpha}_2(T)$ are calculated at $T = (-60, -40, \ldots, 140, 160, 165)^o C$ by simulating the heating of the unit cell by $\Delta T = 2^o C$ from zero-strain state at each value of temperature. The instantaneous effective CTEs $\alpha_1(T)$ and $\alpha_2(T)$ are calculated by simulating cooling process from 165$^o C$ to -60$^o C$ and calculating derivatives of the thermal strains.

Figure 2 presents comparison between effective coefficient of thermal expansion obtained using conventional approach ($\bar{\alpha}_1(T)$ and $\bar{\alpha}_2(T)$ from eq. (8)) and including cooling from curing ($\alpha_1(T)$ and $\alpha_2(T)$ from eq. (10)). CTEs in directions 1 and 2 only are evaluated because the material properties of the reinforcement in the 3rd direction are resin-dominated which leads to a negligible difference between mean and instantaneous CTEs predictions. The temperature range is $-60^o C \leq T \leq 165^o C$ since the original 3D woven composite is cured at 165$^o C$ and can be used at -60$^o C$ for 787 Dreamliner main landing gear brace. It is evident that the two methods provide different results in the considered temperature range, $\bar{\alpha}_1$ is up to 31% smaller than α_1 (comparing to α_1) and $\bar{\alpha}_2$ is up to 9.2% smaller than α_2 as compared to α_2. The difference decreases with increase in temperature and vanishes at 165$^o C$ where cooling starts.

TABLE II. Material parameters for RTM6 epoxy resin.

$E_m^{0^o C}$, MPa	β_m, MPa/^{o}C	$\alpha_m^{0^o C}$, 1/^{o}C	γ_m1/^{o}C^2
3500	5.9	5 × 10^{-5}	-1.05 × 10^{-7}

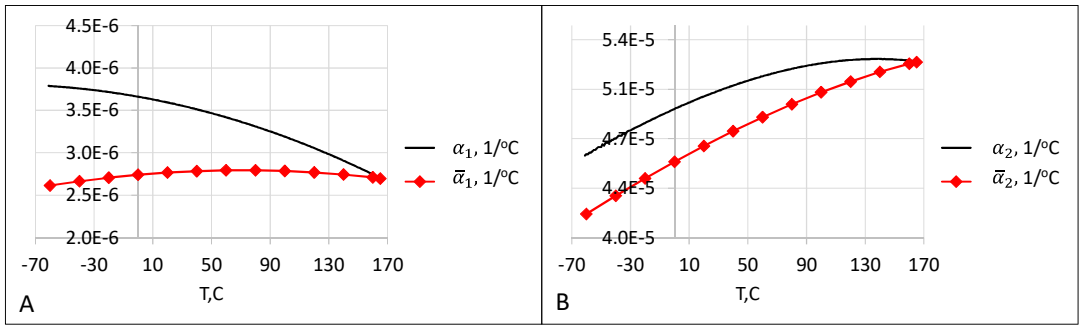

Figure 2. Comparison between effective CTEs in directions (A) 1 and (B) 2 obtained by conventional approach ($\bar{\alpha}_1(T)$ and $\bar{\alpha}_2(T)$) and accounting cooling from curing ($\alpha_1(T)$ and $\alpha_2(T)$).

This is explained by the fact that the composite material consists of two phases with different elastic and thermal properties and most importantly, the elastic properties of one of the phases are temperature dependent. In this particular case, the Young's modulus of the resin varies linearly with temperature. Thus, as the composite deforms due to a uniform temperature change, the values of thermal strain and its derivative are influenced by varying interaction between phases to preserve continuity of the displacement field. This variable interaction is not included in equations (6), (8), or (9).

To confirm that the temperature variation of the elastic properties is the sole factor causing the discrepancy observed in Figure 2, a separate study was performed. A set of similar simulations was carried out for the composite shown in Figure 1 with constant Young's modulus of the matrix phase $E_m = 3854\ MPa$ corresponding to the modulus of the RTM6 resin at -60^oC. All other constituents' properties are kept the same as in the previous study. For a brevity reason, results for direction 1 only are presented.

Figure 3 (A) shows thermal strain in direction 1 as predicted for the composite with E_m varying with temperature *vs.* being a constant value.

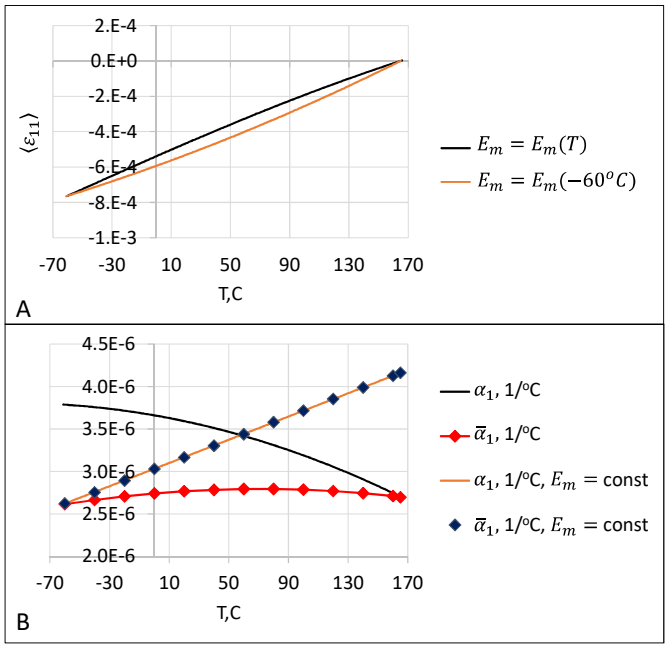

Figure 3. Comparison of (A) thermal strain and (B) effective CTE as obtained using constant value of matrix Young's modulus E_m and as a function of temperature.

As seen in the Figure 3 (B), if the elastic properties of the phases are independent of temperature, both equations (8) and (10) give the same value for effective CTEs. This confirms the assumption that for the elastic properties varying with temperature, prediction of overall CTEs of the composite material will be incorrect if zero-strain state is assumed at each value of temperature and not at the reference state (165^oC in this case).

Effective CTE of 3D Woven Composites with Constituents' Properties Varying with T

Calculation of effective CTEs by differentiation of corresponding components of a thermal strain tensor can be computationally challenging for composite unit cells containing a large number of finite elements as it requires significant computational effort to calculate thermal strain variation within the entire temperature range of interest. We propose an alternative approach to determine effective CTEs accounting for the variation of the elastic moduli with temperature and avoiding calculation of the thermal strain derivatives. It requires to perform direct FE simulations including cooling of the composite from the reference temperature (when the thermal strain is zero). For example, to calculate the effective CTEs at temperature T^* for the 3D woven composite considered in this research, one would need to simulate a cooling down or heating up from $T_{ref} = 165^oC$ to $T_0 = \left(T^* - {}^{\Delta T}/_2\right)$ and sequential heating to $T_1 = \left(T^* + {}^{\Delta T}/_2\right)$. Then the effective CTE is calculated as follows (e.g., modifying equation (8)):

$$\alpha_{ij}(T^*) = \frac{\langle \varepsilon_{ij} \rangle_{T_{ref} \to T_1} - \langle \varepsilon_{ij} \rangle_{T_{ref} \to T_0}}{\Delta T} \tag{11}$$

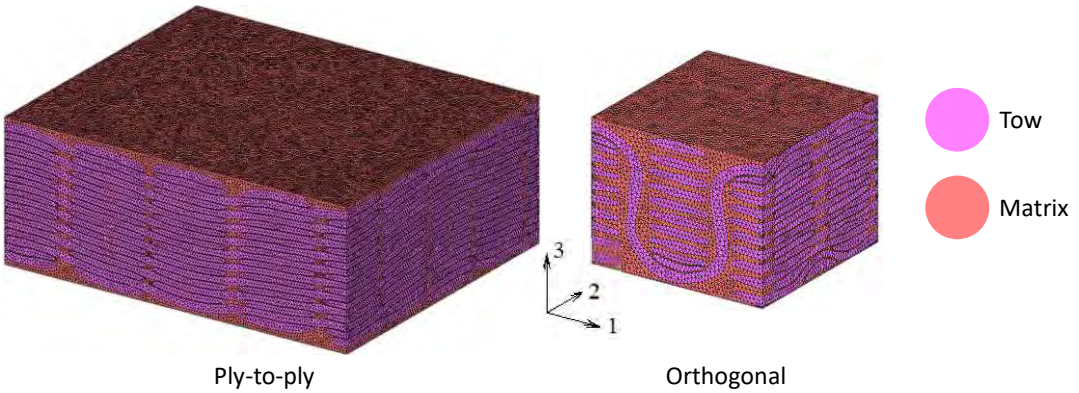

Figure 4. FE meshes of ply-to-ply and orthogonal composites' unit cells.

This allows to avoid calculation of the entire thermal strain evolution while letting account for the variation of constituents' elastic properties with temperature. Equation (11) is used to obtain effective CTEs for two different 3D woven composites: orthogonal and ply-to-ply. The results are compared to the effective CTE values obtained using equation (8) to estimate the discrepancy between the two predictions: when cooling/heating from T_{ref} is taken into account and when thermal strain is assumed to be zero at each value of T_0.

Figure 4 shows FE meshes for the unit cells of 3D woven composite materials with ply-to-ply and orthogonal reinforcement architecture. These FE models were initially developed to evaluate effective elastic response of these composites [17], [35], and predict accumulation of manufacturing-induced residual stresses [15] [16].

TABLE III provides information on volume fractions of the composite reinforcement. The reinforcement consists of two and three types of the tows for ply-to-ply and orthogonal reinforcement, respectively. The types are warp (along direction 1), weft (along direction 2) and binder (through-thickness reinforcement), see Figure 5.

The elastic and thermal properties of the resin-impregnated carbon fiber tows are given in TABLE I and properties of the matrix phase are defined by equations (4) and (5) with material parameters provided in TABLE II. The local material orientation of the tows is prescribed in a way that direction $1'$ corresponds to the longitudinal direction of the tow and directions $2'$ and $3'$ are in the transverse plane.

TABLE III. Tows volume fractions for ply-to-ply and orthogonal composites (PPI stands for picks per inch describing number of warp and weft columns within a single unit cell)

			V_t, %		
Architecture		PPI	Warp	Weft	Binder
Ply-to-ply		12x10	37.57	35.08	-
Orthogonal		10x10	31.65	26.82	7.37

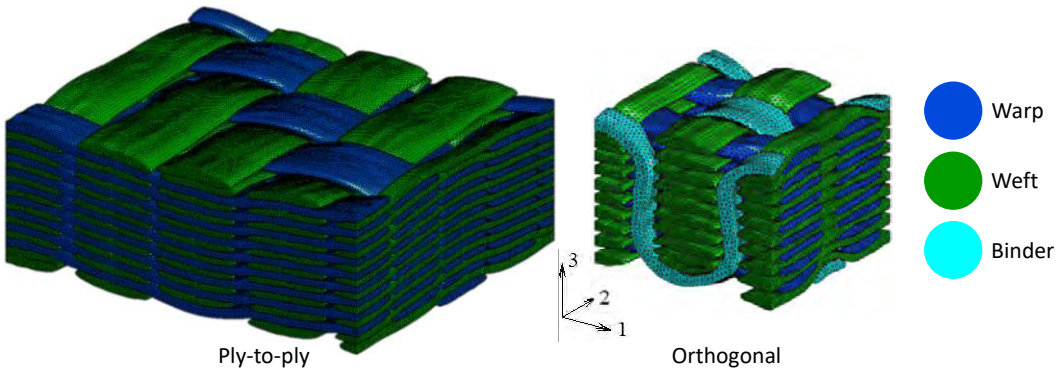

Figure 5. FE meshes of tows of ply-to-ply and orthogonal reinforcements.

Finite element meshes of both reinforcement morphology unit cells have congruent mesh on the opposite sides of the unit cells in directions 1 and 2 to allow application of periodic boundary conditions (Eq. (1)). The unit cells are allowed to contract or expand freely due to the uniform temperature change preserving periodicity of the surface displacements. The model of ply-to-ply composite consists of 5,548,316 linear tetrahedral elements and the orthogonal composite model consists of 672,872 quadratic tetrahedral finite elements.

Effective CTEs of both composites are calculated using formulae (8) and (11) in the temperature range from $-60^{o}C$ to $100^{o}C$ which is a typical range for the service temperature of these composites. Figure 6 shows prediction of effective CTEs in all three directions for ply-to-ply composite material. Similarly to the effective CTEs prediction for the simple composite material (Figure 1), there is a substantial discrepancy between predictions for CTE in directions 1 (up to 16.5%) and 2 (up to 15.7%) and small difference between predictions for CTE in direction 3 (0.1%).

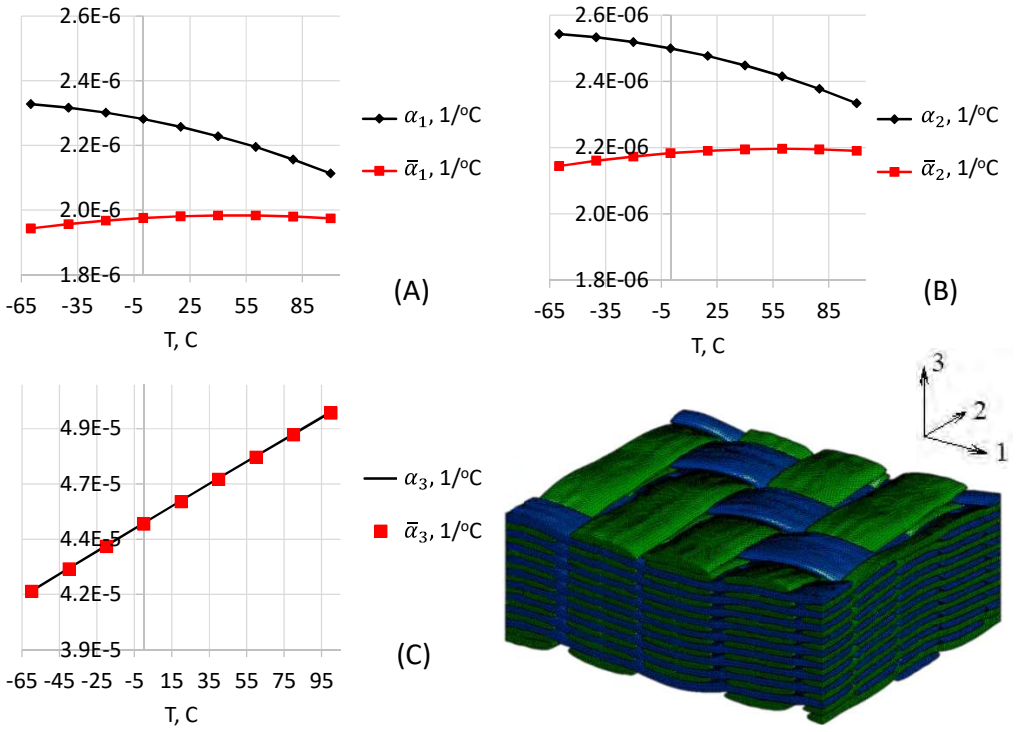

Figure 6. Effective CTEs in (A) first, (B) second and (C) third directions for the ply-to-ply composite as predicted using equations (8) and (11).

This discrepancy can be explained by the fact that if cooling or heating from curing temperature is not taken into account, the variation of the resin's elasticity modulus with temperature is neglected. This becomes important only in case of composites with temperature-dependent elasticity parameters because for homogeneous materials stiffness does not influence thermal strain at all and for composites with temperature-independent constituents the influence (mechanical interaction between phases) on thermal strain is constant at any temperature. The magnitude of the discrepancy depends on the difference between CTEs of the phases: if the difference is small, then thermal behavior of the composite is going to be close to homogeneous material and mechanical interaction between phases would not be important. This is confirmed by comparably small difference of 0.1% between α_3 and $\bar{\alpha}_3$ (Figure 6 (C)) as ply-to-ply composites have lower through-thickness reinforcement if, for example, comparing to orthogonally reinforced materials. Thus, the thermal behavior in the out-of-plane direction is governed mostly by resin properties as tows' elastic and thermal properties in transverse direction are similar to the ones of resin. Additionally, the discrepancy depends on how strong the temperature variation of the elastic properties of the phases is.

Figure 7 shows prediction of effective CTEs in all three directions for orthogonally reinforced composite material. Similarly to ply-to-ply material, the cooling from curing temperature has to be taken into account when calculating effective CTEs. The effective CTEs in directions 1 and 2 are predicted to be up to 16.9% and 15.4% lower if cooling is not included.

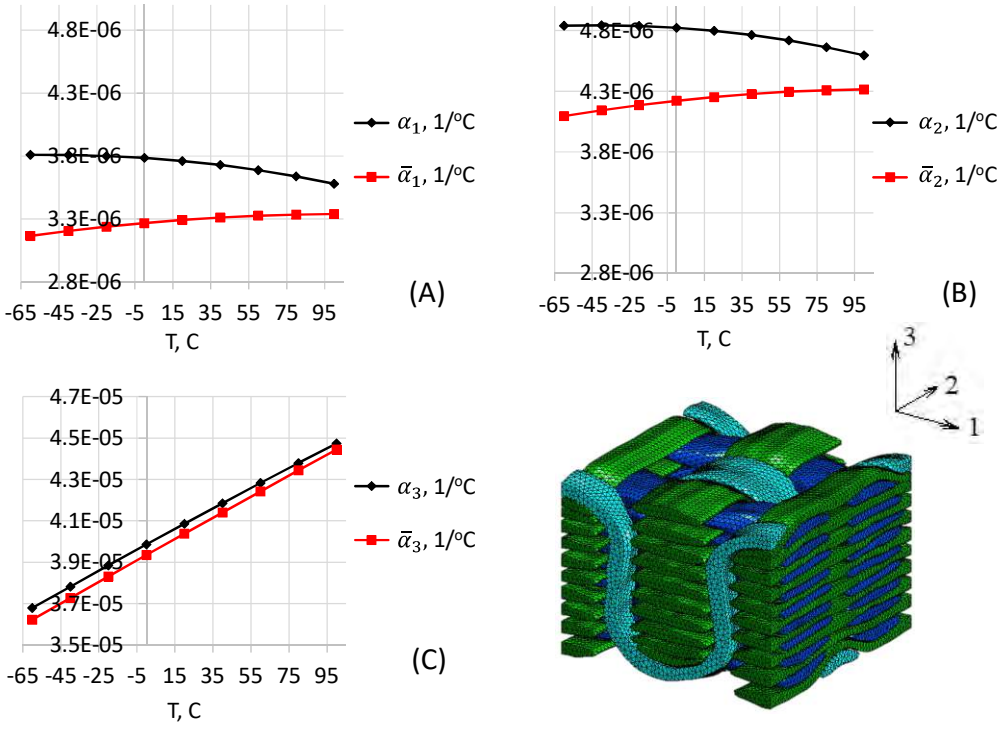

Figure 7. Effective CTEs in (A) first, (B) second and (C) third directions for the orthogonal composite as predicted using equations (8) and (11).

Unlike for the ply-to-ply composite, the discrepancy between α_3 and $\bar{\alpha}_3$ is more noticeable and reaches 1.5%. This is due to more significant level of through-thickness reinforcement.

Generally, both composites show similar thermal behavior. Predicted CTEs are nonlinearly dependent on temperature, α_3 is larger than α_1 and α_2 which is explained by the low amount of through-thickness reinforcement as compared to volume fractions of tows in-plane. For both reinforcements $\alpha_1 < \alpha_2$ as volume fractions of warp tows are larger in both cases. Comparing α_1 for ply-to-ply and orthogonal composites, the effective CTE in this direction is lower for ply-to-ply reinforcement as volume fraction of warp tows is higher compared to the orthogonal reinforcement. Similar trend is observed in direction 2: higher volume fraction of tows → lower CTE.

CONCLUSIONS

Mesoscale FE models can be utilized to predict effective coefficients of thermal expansion of 3D woven composites. It has been shown that, to accurately predict effective CTEs using direct FE simulations, the cooling from curing to the temperature of interest must be taken into account, otherwise CTEs can be underpredicted and the farther the temperature of interest from curing temperature the larger the magnitude of error can be. The cooling/heating from curing should be taken into account if elastic properties of the phases vary with temperature and this variation is significant. It has been observed that this effect is not significant if the volume fraction of reinforcement is low (e.g., out-of-plane direction for considered

3D woven composites). It has also been shown that thermal behavior of 3D woven composite can become nonlinear even with linearly varying constituents' elastic and thermal properties due to the interaction between the phases.

The correlation of the effective CTEs of carbon-fiber/epoxy 3D woven composites with volume fraction of the reinforcement is observed, namely the larger the volume fraction of a particular type of tows the lower the effective CTE in this direction. It has been shown that addition of through-thickness reinforcement can not only tailor elastic and fracture properties in out-of-plane direction but the overall CTE as well. For the fibrous 3D woven composites, the larger the amount of reinforcement in out-of-plane direction, the lower the effective CTE in the same direction.

ACKNOWLEDGEMENTS

This material is based upon work supported by the National Science Foundation under Grant No. CMMI-1662098.

REFERENCES

[1] Huang T, Wang Y, Wang G. Review of the Mechanical Properties of a 3D Woven Composite and Its Applications. Polym Plast Technol Eng 2018;57:740–56. https://doi.org/10.1080/03602559.2017.1344857.

[2] Tan P, Tong L, Steven GP, Ishikawa T. Behavior of 3D orthogonal woven CFRP composites. Part I. Experimental investigation. Compos Part A Appl Sci Manuf 2000;31:259–71. https://doi.org/10.1016/S1359-835X(99)00070-6.

[3] Ikarashi Y, Ogasawara T, Aoki T. Effects of cyclic tensile loading on the rupture behavior of orthogonal 3-D woven SiC fiber/SiC matrix composites at elevated temperatures in air. J Eur Ceram Soc 2019;39:806–12. https://doi.org/10.1016/j.jeurceramsoc.2018.10.016.

[4] Ma Z, Zhang P, Zhu J. Review on the fatigue properties of 3D woven fiber/epoxy composites: testing and modelling strategies. J Ind Text 2020. https://doi.org/10.1177/1528083720949277.

[5] Islam MS, Melendez-Soto E, Castellanos AG, Prabhakar P. Investigation of woven composites as potential cryogenic tank materials. Cryogenics (Guildf) 2015;72:82–9. https://doi.org/10.1016/j.cryogenics.2015.09.005.

[6] Wilkinson MP, Ruggles-Wrenn MB. Fatigue of a 3D Orthogonal Non-crimp Woven Polymer Matrix Composite at Elevated Temperature. Appl Compos Mater 2017;24:1405–24. https://doi.org/10.1007/s10443-017-9597-5.

[7] Sevostianov I. On the thermal expansion of composite materials and cross-property connection between thermal expansion and thermal conductivity. Mech Mater 2012;45:20–33. https://doi.org/10.1016/j.mechmat.2011.10.001.

[8] Tan P, Tong L, Steven GP. Models for Predicting Thermomechanical Properties of Three-Dimensional Orthogonal Woven Composites. J Reinf Plast Compos 1999;18:151–85. https://doi.org/10.1177/073168449901800204.

[9] Ai S, Fu H, He R, Pei Y. Multi-scale modeling of thermal expansion coefficients of C/C composites at high temperature. Mater Des 2015;82:181–8. https://doi.org/10.1016/j.matdes.2015.05.061.

[10] Wang P, Zhang S, Li H, Kong J, Li W, Zaman W. Variation of thermal expansion of carbon/carbon composites from 850 to 2500°C. Ceram Int 2014;40:1273–6. https://doi.org/10.1016/j.ceramint.2013.08.038.

[11] Dong K, Peng X, Zhang J, Gu B, Sun B. Temperature-dependent thermal expansion behaviors of carbon fiber/epoxy plain woven composites: Experimental and numerical studies. Compos Struct 2017;176:329–41. https://doi.org/10.1016/j.compstruct.2017.05.036.

[12] Gou JJ, Gong CL, Gu LX, Li S, Tao WQ. The unit cell method in predictions of thermal expansion properties of textile reinforced composites. Compos Struct 2018;195:99–117.

https://doi.org/10.1016/j.compstruct.2018.04.045.
[13] Siddgonde N, Ghosh A. Thermo-mechanical modeling of C/C 3D orthogonal and angle interlock woven fabric composites in high temperature environment. Mech Mater 2020;148:103525. https://doi.org/10.1016/j.mechmat.2020.103525.
[14] Trofimov A, Le-Pavic J, Therriault D, Lévesque M. An efficient multi-scale computation of the macroscopic coefficient of thermal expansion: Application to the Resin Transfer Molding manufactured 3D woven composites. Int J Solids Struct 2021;210–211:162–9. https://doi.org/10.1016/j.ijsolstr.2020.11.012.
[15] Drach B, Tsukrov I, Trofimov A, Gross T, Drach A. Comparison of stress-based failure criteria for prediction of curing induced damage in 3D woven composites. Compos Struct 2018;189:366–77. https://doi.org/10.1016/j.compstruct.2018.01.057.
[16] Vasylevskyi K, Tsukrov I, Drach B, Buntrock H, Gross T. Identification of process-induced residual stresses in 3D woven carbon/epoxy composites by combination of FEA and blind hole drilling. Compos Part A Appl Sci Manuf 2020;130:105734. https://doi.org/10.1016/j.compositesa.2019.105734.
[17] Drach A, Drach B, Tsukrov I. Processing of fiber architecture data for finite element modeling of 3D woven composites. Adv Eng Softw 2014;72:18–27. https://doi.org/10.1016/j.advengsoft.2013.06.006.
[18] Wang Y, Sun X. Digital-element simulation of textile processes. Compos Sci Technol 2001;61:311–9. https://doi.org/10.1016/S0266-3538(00)00223-2.
[19] Lomov S V, Ivanov DS, Verpoest I, Zako M. Meso-FE modelling of textile composites : Road map, data flow and algorithms. Compos Sci Technol 2007;67:1870–91. https://doi.org/10.1016/j.compscitech.2006.10.017.
[20] Zhou E, Mollenhauer D, Iarve E. A realistic 3-D textile geometric model. Seventeenth Int Conf Compos Mater ICCM-17 2009:100–10.
[21] Long AC, Brown LP. 8 - Modelling the geometry of textile reinforcements for composites: TexGen. In: Boisse P, editor. Compos. Reinf. Optim. Perform., Woodhead Publishing; 2011, p. 239–64. https://doi.org/https://doi.org/10.1533/9780857093714.2.239.
[22] Miao Y, Zhou E, Wang Y, Cheeseman BA. Mechanics of textile composites : Micro-geometry. Compos Sci Technol 2008;68:1671–8. https://doi.org/10.1016/j.compscitech.2008.02.018.
[23] Whitcomb JD, Chapman CD, Tang X. Derivation of Boundary Conditions for Micromechanics Analyses of Plain and Satin Weave Composites. J Compos Mater 2000;34:724–47. https://doi.org/10.1177/002199830003400901.
[24] Tsukrov I, Giovinazzo M, Vyshenska K, Bayraktar H, Goering J, Gross T. Comparison of Two Approaches to Model Cure-Induced Microcracking in Three-Dimensional Woven Composites. Vol. 3 Des. Mater. Manuf. Parts A, B, C, ASME; 2012, p. 541. https://doi.org/10.1115/IMECE2012-86395.
[25] Chamis CC. Mechanics of composite materials: Past, present, and future. J Compos Technol Res 1989;11:3–14. https://doi.org/10.1520/ctr10143j.
[26] Tsukrov I, Bayraktar H, Giovinazzo M, Goering J, Gross T, Fruscello M, et al. Finite element modeling to predict cure-induced microcracking in three-dimensional woven composites. Int J Fract 2011;172:209–16. https://doi.org/10.1007/s10704-011-9659-x.
[27] Tsukrov I, Drach B, Gross T. Effective stiffness and thermal expansion coefficients of unidirectional composites with fibers surrounded by cylindrically orthotropic matrix layers. Int J Eng Sci 2012;58:129–43. https://doi.org/10.1016/j.ijengsci.2012.03.032.
[28] Hashin Z, Shtrikman S. A variational approach to the theory of the elastic behaviour of multiphase materials. J Mech Phys Solids 1963;11:127–40. https://doi.org/10.1016/0022-5096(63)90060-7.
[29] Hashin Z. Analysis of Properties of Fiber Composites With Anisotropic Constituents. J Appl Mech 1979;46:543–50. https://doi.org/10.1115/1.3424603.
[30] Schapery RA. Thermal Expansion Coefficients of Composite Materials Based on Energy Principles. J Compos Mater 1968;2:380–404. https://doi.org/10.1177/002199836800200308.
[31] Brauner C, Block TB, Purol H, Herrmann AS. Microlevel manufacturing process simulation of carbon fiber/epoxy composites to analyze the effect of chemical and thermal induced residual stresses. J Compos Mater 2012;46:2123–43. https://doi.org/10.1177/0021998311430157.
[32] Karch C. Micromechanical Analysis of Thermal Expansion Coefficients. Model Numer Simul

Mater Sci 2014;04:104–18. https://doi.org/10.4236/mnsms.2014.43012.
[33] Drach B, Tsukrov I, Trofimov A. Comparison of full field and single pore approaches to homogenization of linearly elastic materials with pores of regular and irregular shapes. Int J Solids Struct 2016;96:48–63. https://doi.org/10.1016/j.ijsolstr.2016.06.023.
[34] Morelle XP, Chevalier J, Bailly C, Pardoen T, Lani F. Mechanical characterization and modeling of the deformation and failure of the highly crosslinked RTM6 epoxy resin. Mech Time-Dependent Mater 2017;21:419–54. https://doi.org/10.1007/s11043-016-9336-6.
[35] Ewert A, Drach B, Vasylevskyi K, Tsukrov I. Predicting the overall response of an orthogonal 3D woven composite using simulated and tomography-derived geometry. Compos Struct 2020;243:112169. https://doi.org/10.1016/j.compstruct.2020.112169.